Structural properties and biological activities of collagens from four main processing by-products (skin, fin, cartilage, notochord) of sturgeon *(Acipenser gueldenstaedti)*

Dawei Meng[a*], Qiwei Wei[b], Yasuaki Takagi[c], Zhiyuan Dai[a], Yan Zhang[d]

a Zhejiang Province Joint Key Laboratory of Aquatic Products Processing, Institute of Seafood, Zhejiang Gongshang University, 149 JiaoGong Road, Hangzhou 310012, China

b Key Laboratory of Freshwater Biodiversity Conservation, Ministry of Agriculture and Rural Affairs, Yangtze River Fisheries Research Institute, Chinese academy of Fishery Sciences, Wuhan, 430223, China

c Faculty of Fisheries Sciences, Hokkaido University, 3-1-1 Minato-cho, Hakodate, Hokkaido 041-8611, Japan

d Liangzhu laboratory, Zhejiang University Medical Center, Hangzhou 310058, Zhejiang, China

Corresponding author at: Zhejiang Province Joint Key Laboratory of Aquatic Products Processing, Institute of Seafood, Zhejiang Gongshang University, Hangzhou 310012, China.

E-mail addresses: dawei@mail.zjgsu.edu.cn (D. Meng)

Abstract

During the processing of sturgeon, large amounts of by-products, such as skin, fin, cartilage, and notochord, are produced. These by-products have not been effectively used, resulting in a serious waste of sturgeon resources. In this study, we aimed to obtain the collagen from these by-products and evaluate the fibril-forming characteristics of the collagen molecules and the antioxidant activity of the collagen peptides. The structural properties of pepsin-soluble collagen were analyzed by SDS-PAGE and FTIR. Collagen fibril-forming characteristics were detected by turbidity assay and SEM observation. The antioxidant activities of collagen peptides were determined by Hydroxyl and ABTS radical scavenging assays. SDS-PAGE results showed that the skin and fin collagens were characterized as type I collagen, and the cartilage and notochord collagens were characterized as type II collagen. Sturgeon type II collagens could only be self-assembled into fibrils at low phosphate ion concentration, whereas sturgeon type I collagens could be self-assembled into fibrils at long range of phosphate ion concentrations. The fibril-forming ability of sturgeon type I collagen was higher than that of porcine type I collagen. The fibril diameter of type I collagen was higher than that of type II collagen. The antioxidant activity of notochord and skin collagen peptides was higher than that of the other two collagen peptides. The results of this study will provide helpful information for the application of sturgeon collagen in the functional food and biomedical material industries. Meanwhile, it will promote the effective use of collagen from different sturgeon by-products.

Graphical abstract

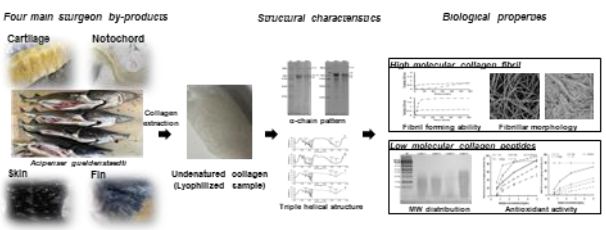

Keyword: Sturgeon by-products; Collagen; Structural properties; Fibril-forming characteristics; Collagen peptides; Antioxidant activity

Statement of Novelty

In China, more than 16,000 tons of female sturgeon are used for caviar production. After roe retrieval, collagen-rich by-products, which are not suit for edible, will be produced during the processing of fish. This work was the first to clarify and compare structural properties of collagen extracted from four main by-products (fin, skin, notochord, cartilage) of sturgeon in one research. Furthermore, this work was the first to discuss the biological properties of sturgeon collagen from high molecular collagen fibril and low molecular collagen peptides, respectively. The results of this study will provide helpful information of sturgeon collagens in different by-products. Meanwhile, according to its own functional characteristics, different collagen will be used reasonably and effectively in a suitable field.

Introduction

Sturgeon is an economically valuable fish known for its caviar. Due to overfishing and destruction of the living environment, since 1997 all wild sturgeons have been listed as critically endangered and protected species by the International Union for Conservation of Nature [1]. To meet the demand for caviar and reduce the pressure on wild sturgeon, aquaculture industry has developed rapidly in the past 20 years. The total global harvest of farmed sturgeon increased from 18,000 ton in 2003 to more than 102,000 ton in 2019 [2]. China is the biggest sturgeon farming and caviar producing country in the world. In 2017, the aquaculture volume of sturgeon in China exceeded 80,000 tons, accounting for 85% of the world's total production; the output of caviar exceeded 100 tons, accounting for 78% of the world's total production [2, 3]. Currently, approx. 20% of China's total sturgeon production is the large

67 females that produces caviar.

68 Russian sturgeon *(Acipenser gueldenstaedti)* is one of species of sturgeon native to the sea area at
69 the junction of Asia and Europe [4]. In current, it is a commercial sturgeon species accounting for 10%
70 of the annual production of sturgeon in China [5, 6]. The main purpose of Russian sturgeon farming is
71 to produce caviar. Since it takes more than 10 years to obtain roe, Russian sturgeon is more expensive
72 to farm than other fishes, including hybrid sturgeon. After egg retrieval, these large fish bodies (over
73 1.5 meters) are divided into several parts for further processing. During the production process, huge
74 amounts of inedible by-products, such as head, skin, bone, fin, and viscera, are produced. These by-
75 products are not suitable for consumption and represent up to more than 70% of the total fish body. In
76 the past, sturgeon by-products were often discarded as waste or used as material for direct feeding in
77 aquaculture and raising of livestock and fur animals in China. As known, discarding these sturgeon by-
78 products will aggravate the problem of environmental pollution. The lack of efficient use of these by-
79 products other than caviar limits the profitability of aquaculture industry and leads to waste of fish
80 sources. Efficient utilization of these by-products will increase the value of Russian sturgeon, create
81 more economic benefits, and promote the development of sturgeon aquaculture. Meanwhile, it will
82 avoid wasting Russian sturgeon resources. Previous studies have shown that some sturgeon by-
83 products contained a variety of bioactive collagens [7, 8, 9].

84 Collagen is a main structural protein in the connective tissue of living organism [11]. *In vivo*,
85 collagen interacts with other components, such as proteoglycan and other proteins, to form a stable
86 network of fibrils. This fibrillar structure provides an appropriate growth environment for cells and
87 affects cellular functions [9]. *In vitro*, fibrillar collagen molecules can self-assemble into fibrils that
88 reassemble native tissue forms under suitable conditions [10]. Due to this special biological property,

89 collagen is widely used as biomedical materials to repair or replace damaged or diseased human tissues
90 and organs. In recent years, with the increasing demand for high value-added utilization of aquatic
91 waste, more and more researches on fish collagen have been conducted [9]. With no zoonotic risks and
92 religious restrictions, fish by-products are considered as a safe natural source of collagen [11, 12]. Our
93 recent studies have reported the biochemical characteristics and fibril-forming properties of collagen
94 from hybrid sturgeon (*Huso huso* × *Acipenser ruthenus*) skin, swim bladder, and notochord [7, 8, 13].
95 We found that different tissues contained different types of collagens and that there were significant
96 differences in the fibril-forming ability of collagen in tissues specific. For example, collagen extracted
97 from sturgeon swim bladder and skin was type I collagen, while collagen extracted from sturgeon
98 notochord was type II collagen [7, 8]. Although both swim bladder and skin collagen were type I
99 collagen, the fibril-forming ability and fibril morphology of two collagens were significant different
100 [13]. The *in vitro* fibril-forming ability is closely related to the application of collagen in biomedical
101 materials. In addition, the morphological characteristics of collagen fibrillar materials, including their
102 diameter, shape, and orientation, have a determining influence on the adhesion, alignment,
103 proliferation, and differentiation of anchorage-dependent cells [14]. Therefore, in order to utilize
104 collagens from different Russian sturgeon by-products, it is necessary to clarify and compare the
105 structural properties and fibril-forming properties of collagens in different tissues. To our knowledge,
106 no previous study has reported the *in vitro* fibril-forming properties of Russian sturgeon collagens.
107 On the other hand, low molecular collagen peptides attracted high attention of researchers because
108 of their various bioactivities, such as antioxidant, antihypertensive, antimicrobial, anticancer activities,
109 and so on [15]. Due to these bioactivities, collagen peptides are used as functional ingredient additives
110 in health foods and cosmetics. In aerobic organisms, reactive oxygen species (ROS) with a high

reaction activity, including hydroxyl radical, superoxide anion radical, hydrogen peroxide, and singlet oxygen, are generated during the metabolism [16]. In general, cellular antioxidases, such as superoxide dismutase, glutathione peroxidase, and catalase, can keep ROS in a state of balance [17]. Ultraviolet irradiation, aging, stress, environmental deterioration, and other reasons can disrupt the balance, and excess ROS in the body can induce enzyme inactivation, polysaccharide depolymerization, DNA cleavage, and cell membrane destruction [17]. Till now, amounts of studies have been conducted on the antioxidant activity of collagen peptides from fish tissues [18]. For sturgeon, some studies have investigated the antioxidant activity of collagen peptides from their skin and cartilage [19, 20]. However, there was no study on the antioxidant activity of collagen peptides from notochord and fin. Furthermore, the antioxidant activity of different types of collagen peptides, such as type I and II collagen peptides, have never been compared in previous studies.

The aim of this study was to clarify the structural properties of collagen extracted from four main by-products of Russian sturgeon, and to evaluate the fibril-forming characteristics of the four collagen molecules and the antioxidant activity of the four collagen peptides. Firstly, we extracted pepsin-soluble collagen from the four main by-products of fin, skin, backbone cartilage, and notochord in the same method. Then, we evaluated *in vitro* fibril-forming properties of collagen molecules using turbidity assay and SEM observation. Finally, we compared the antioxidant activities of collagen enzymatic hydrolysates using ABTS and Hydroxyl radical-scavenging assays. The results of this study will clarify the properties of collagen from the four main by-products and promote the efficient utilization of collagen in different tissues of Russian sturgeon. Meanwhile, it will provide helpful information for the application of Russian sturgeon collagen in the biomedical material and functional food industries.

Materials and methods

Isolation and purification of collagen

The fin, skin, backbone, and notochord of the Russian sturgeon *(Acipenser gueldenstaedti)* after spawning were obtained from the Sturgeon Biological Technology Co. Ltd. (Xinchang county, Zhejiang province, China). The samples were washed with chilled tap water, and lyophilized in a freeze dryer (FreeZone 2.5 L, American Labconco Co, Ltd, Kansas City, USA). The fat of backbone cartilage, fin, and skin was removed over 24 h in anhydrous ethanol (two solution-changes) at 4 °C, with a sample : solution ratio of 1:10 (w/v). Defatted samples and notochord sheath were cut into small pieces for collagen extraction. Due to antigenic telopeptides existing at both ends of the collagen molecule, acid-soluble collagen may not be suitable for direct use as biomaterials [21]. Pepsin can cleave the peptides in the telopeptide region in extraction process [22]. In this study, we focused on pepsin-soluble collagen from sturgeon by-products. Isolation and purification progress of pepsin-soluble collagen were performed according to the procedures reported by our previous method [8, 23]. Porcine skin and bovine cartilage collagens were used to compare the structural properties and biological activities of Russian sturgeon collagens. The samples were obtained from Fuyang Jiuxian Beef Slaughtering Co. Ltd. (Hangzhou, Zhejiang province, China). The pepsin-soluble collagen extraction method was the same as above.

Sodium dodecyl sulfate-polyacrylamide gel electrophoresis (SDS-PAGE)

SDS-PAGE was performed according to the method of Laemmli [24]. The lyophilized collagen was dissolved in pH 2.0 HCl at a concentration of 1 mg/ml. The collagen samples were mixed at a ratio of 1:1(v/v) with sample buffer (0.5 M Tris-HCl buffer, pH 6.8, with 4% SDS and 20% glycerol) containing 10% β-mercaptoethanol. The mixed solution was boiled for 3 min. Ten micrograms of

mixture were loaded onto each lane. Electrophoresis was performed at 15 mA for the stacking gel and 25 mA. Collagen molecule electrophoresis was running with the 8% running gel, collagen enzymatic hydrolysates was running with the 15% running gel. After electrophoresis, the gel was stained for 30 min with a 0.1% Coomassie Brilliant Blue R250 solution and de-stained with a mixture of 20% methanol, 5% acetic acid, and 2.5% glycerin.

Fourier-transform infrared (FTIR) spectroscopy analysis

FTIR spectroscopy of collagen was recorded with an infrared spectrophotometer (Nicolet iS10, Thermo Scientific, Madison, USA). The collagen powder was ground together with potassium bromide (w/w 1:200), and then pressed into a 1 mm pellet for measurement in the spectra range of 500-4000 cm^{-1}. The potassium bromide powder was used as the background.

Solubility of collagen in different pH

The solubility of collagen was measured using the method proposed by Atef et al [25]. with a slight change. Dry collagen was dissolved in aqueous solutions with different pH (2, 4, 6, 8, 10, 12) to 3mg/ml. The collagen solution was shake for 12 h at 21 °C. Then, each collagen solution was centrifugated at 20,000 ×*g* for 20 min at 4 °C, the protein concentration of the supernatant was measured by Lowry method [26], using bovine serum albumin as a standard. The solubility of collagen was defined as the percentage of the collagen concentration in the solution, ie, the solubility of collagen at different pH conditions.

Collagen fibril formation *in vitro*

The fibril formation process of collagen was evaluated by the method of Meng et al [8]. Lyophilized collagen was dissolved in pH 2.0 HCl solution to 0.3% (w/v). The collagen solution was mixed with a Na-phosphate buffer (PB) solution (pH 7.4), having a Na-phosphate concentration of 45, 90, and 180

177 mM, respectively. The collagen solution/PB ratio was set to 1:2 (v/v), which resulted in a final PB
178 concentration of 30 ,60, and 120 mM, respectively. The mixed solution was place into a quartz cuvette,
179 and the subsequent fibril formation at 21°C was monitored by measuring increased turbidity via optical
180 absorbance at 320 nm, using a spectral monitor (Evolution 60 s, Thermo fisher scientific, Waltham,
181 USA). The fibril formation of skin and fin collagen was monitored for 1 h. The fibril formation of
182 backbone and notochord collagen was monitored for 10 h.

183 **Morphology of collagen fibrils**

184 The microstructure of fin and skin collagen fibrils was observed using scanning electron microscope
185 (SEM; Sigma 500, Carl Zeiss Ltd, Germany), as previously described in Meng et al [8]. Collagen fibrils
186 were formed using the same conditions as described above. Sample suspensions were centrifuged at
187 20,000 ×*g* for 20 min at 4 °C to obtain precipitates of collagen fibrils. The fibrils were fixed with 2.5%
188 (v/v) glutaraldehyde in phosphate buffer (pH 7.4) for 3 h at room temperature, rinsed with phosphate
189 buffer to remove the fixative, dehydrated with a graded series of ethanol solutions, and then soaked in
190 two 30-min changes of t-butyl alcohol solution. Finally, collagen fibrils were freeze-dried in a t-butyl
191 alcohol solution with a freeze-drying device and coated with gold-platinum using an auto fine coater
192 (JFC-1600; JEOL Ltd.). After the SEM observations, digital images of the sample were taken, and the
193 diameters of 100 randomly selected fibrils were determined using the software ImageJ. The
194 measurements were performed three times using different photographs.

195 **Degree of fibril formation**

196 The fibril formation degree was determined followed by the method of Zhang et al [7]. After fibril
197 formation, the mixture was centrifugated at 20,000 ×*g* for 20 min at 4 °C, the protein concentration of
198 the supernatant was measured by Lowry method [26], using bovine serum albumin as a standard. The

199 degree of fibril formation was defined as the percentage of the decrease of collagen concentration in
200 the solution, which meant the percentage of collagen molecules that formed the fibrils. The fibril
201 formation degree was detected after completion of fibril formation for each sample.

202 **Enzymatic hydrolysis of collagen**

203 Purified collagens were soaked in distilled water with a sample/solution ratio of 1:60 (w/v) at 60 °C for
204 1 h for gelatinization. Papain was used to hydrolyze purified collagens with a concentration of 2.5%
205 (w/w) for 4 h at 50 °C. The reaction was terminated by boiling samples for 10 min. The reaction
206 solution was filtered with cellulose acetate membrane filter (pore size 0.45 μm) remove the
207 unhydrolyzed residues. Then, all hydrolysates were lyophilized and stored at −30 °C until use. The
208 percentage of dry weight of collagen hydrolysate in comparison with dry weight of the initial collagen
209 was calculated as the collagen peptide yield.

210 **Hydroxyl scavenging activity of collagen peptides**

211 Hydroxyl radical scavenging activity was determined according to the method of Pan et al. [27].
212 Briefly, a 1,10-phenanthroline solution (1.0 ml, 1.865 mM) was mixed with 2 ml of the sample
213 solution, and then $FeSO_4 \cdot 7H_2O$ solution (1.0 ml, 0.75 mM) was pipetted into the mixture. The reaction
214 was initiated by adding 1.0 ml of H_2O_2 (0.01% v/v). After incubation at 37°C for 60 min, the
215 absorbance was measured at 536 nm against a reagent blank. The reaction solution without antioxidants
216 was used as a negative control, and the mixture without H_2O_2 was used as the blank. Vitamin C (Vc)
217 was used as positive control. The hydroxyl radical scavenging activity was calculated according to Eq.
218 1:

219 $$\text{Scavenging activity (\%)} = [(As - An) / (Ab - An)] \times 100\%$$

220 where As, An, and Ab are the absorbance values at 536 nm of the sample, negative control, and blank

after the reaction, respectively.

ABTS radical scavenging activity of collagen peptides

The ABTS radical scavenging activity was determined by the method of Re et al. [28]. In brief, ABTS radical cation was generated by mixing the ABTS stock solution (7 mM) with potassium persulfate (2.45 mM). The mixture was left in the dark at room temperature for 16 h. The ABTS radical solution was diluted in 5 mM phosphate buffered saline at pH 7.4 to an absorbance of 0.7 at 734 nm. One milliliter of diluted ABTS radical solution was mixed with 1 ml of different concentrations of samples. Ten minutes later, the absorbance was measured at 734 nm against the corresponding blank. Vc was used as positive control. The ABTS radical scavenging activity of samples was calculated according to Eq. 2:

Scavenging activity (%) = [(Ac – As) / Ac] × 100%

where As and Ac are the absorbances with and without a sample.

Statistical analysis

Each experiment was replicated three times. The data of collagen solubility, fibril formation degree, and radical scavenging activity were expressed as means ± standard errors.

Results and Discussion

SDS-PAGE

The α-chain pattern of collagens was shown in Fig. 1. Fin and skin collagens (Lane 1 and 2) contained two α-chains (approx. 120 kDa and 110 kDa) as the major constitutes and a small amount of β-chain. The major α-chains at 120 kDa and 110 kDa were attributed to the α1(I) or α3(I), and α2(I) of type I collagen, respectively. The molecular weight of sturgeon type I collagen was a little lower than that of porcine skin type I collagen, but they had the similar α-chain pattern (Lane 5). The α-chain pattern of

243 skin collagen in this study was consistent with our previous study on the skin collagen of hybrid
244 sturgeon *(Huso huso* × *Acipenser ruthenus*) [8]. The band of α1(I) in fin collagen was much thicker
245 than that in skin collagen, indicating differences in the molecular structure of fin and skin collagens.
246 Nagai et al. reported that the sea-bass fin collagen was type I collagen, which only contained a single α
247 band [29]. Liu et al. found that bighead carp fin collagen had both α1(I) and α2(I) in a ratio of 2.12
248 [30]. It is well known that type I collagen comprises two α1(I) chains and one α2(I) chain in a ratio of
249 2:1, and its molecular form is $[\alpha1(I)]_2\alpha2(I)$ [31]. Meanwhile, Saito et al. reported that a heterotrimer of
250 type I collagen containing three non-identical α-chains, α1(I) α2(I) α3(I), was found in the skin and
251 muscle collagen of rainbow trout [32]. Since α3(I) and α1(I) had similar molecular weight, they could
252 not be separated by electrophoresis. Low α2(I) was detected by electrophoresis in SDS-PAGE result
253 indicated that the molecular structure of sturgeon fin collagen might contain more triple helical
254 molecules with α-chain patterns of $\alpha1[I]_3$, $\alpha1[I]_2\alpha3[I]$, $\alpha1[I]\alpha3[I]_2$, and $\alpha3[I]_3$. Zhang et al. reported that
255 the ratio of α1/α2 gene expression was higher in the fin than in the skin of Amur sturgeon *(Acipenser*
256 *schrenckii)*. Although different sturgeon species might have different gene expression, the gene
257 expression results was consistent with the SDS-PAGE results of this study [33].
258 The notochord collagen (Lane 3) contained a single major band at approx. 130 kDa, which was
259 the characteristic of type II collagen α-chain [8]. β-chain was not detected in the notochord collagen. A
260 slight high molecular weight band above major α-chain was presumed to be type IX or XI collagen
261 [34]. The α-chain composition of notochord collagen was consistent with that of bovine cartilage
262 collagen (Lane 6). These results were consistent with the α-chain properties of Bester sturgeon (*Huso*
263 *huso* × *Acipenser ruthenus*) notochord collagen [7]. It suggested that the α-chain pattern of notochord
264 collagen was independent of sturgeon species.

The cartilage collagen (Lane 4) contained three α-chains (approx. 130 kDa, 120 kDa and 110 kDa) as the major constituents and a small amount of β-chain. The major α-chain at 130 kDa was attributed to the α1(II) of type II collagen. The other two α-chains (approx.120 kDa and 110 kDa) were corresponded to α1(I) and α2(I) of type I collagen. This result was consistent with the conclusion that type II collagen was the main collagenous component in cartilage tissue [35]. The reason for the presence of type I collagen in backbone was thought to be cartilage ossification. Ossification is a process by which bone form in soft tissues, such as cartilage [36]. Zhang et al. showed that ossification of the spine cartilage was observed in hybrid sturgeon *(H. huso × A. ruthenus)* [37]. Leprévost et al. also reported that bone was deposited around the spine cartilage of Siberian sturgeon *(Acipenser Baerii)* [38]. As known, type I collagen constituted approx. 95% of total collagen in bone [39]. The exact proportion of type I collagen in sturgeon backbone was not known from this study. It might be related to the degree of cartilage ossification. Leprévost et al. found that the bone thickness on the cartilage varied with the region of cartilage and the age of sturgeon [38]. In addition, Zhang et al. reported that gene of ascol1α1 (Col I) and ascol2α1 (Col II) were expressed in sturgeon vertebral cartilage [40]. It demonstrated the presence of type I collagen in sturgeon backbone cartilage by molecular analyses. The results of α-chain patterns in this research were consistent with this finding.

Mizuta et al. and Luo et al. reported that type I collagen was the major collagenous components in the vertebral cartilage of White sturgeon *(Acipenser transmontanus)* and Siberian sturgeon *(Acipenser baeri)* [41, 42]. Liang et al. and Zhu et al. reported that the pepsin-soluble collagens extracted from the cartilage of Hybrid sturgeon *(Acipenser schrencki × Huso dauricus)* and Amur sturgeon *(Acipenser schrenckii)* were type II collagen [34, 43]. The differences in α-chain patterns among sturgeon species were thought to be caused by different extraction processes. In our previous study, we found that type

II collagen was more difficult to extract than type I collagen by the same extraction method [8]. In this research, we stopped the collagen extraction process until there was no residue in the extract. It allowed complete extraction of type I and type II collagen molecules. Since the purification process of two collagens was same, the pepsin-soluble cartilage collagen purified in this study contained both two type collagens. Furthermore, during collagen purification process, the NaCl concentration used might be another reason for obtaining different types of collagens. Because, during salting out process, different type of collagens could be precipitated in a biological tissue using different concentrations of NaCl [44]. In fact, we found that in the current studies, the NaCl concentrations used to isolate the sturgeon cartilage collagen were all different in these studies [34, 41, 42, 43].

FTIR spectroscopic analysis

The FTIR spectra was presented in Fig. 2. showing the intact triple helical structure in collagens. According to Plepis et al [45], the ratio of absorbance of amide III to peak between 1400 to 1454 cm^{-1} wavelength is close to 1.0, indicating that the triple helical structure of collagen is intact. In this study, the ratios of fin, skin, notochord, and cartilage collagen were 0.97, 1.05, 1.01 and 0.99, respectively. The ratios of porcine skin and bovine cartilage collagen were 1.00 and 0.99, respectively. It indicated that the complete triple helical structure was retained in all collagens. Otherwise, the main characteristic absorption peaks of collagen contained amide A, amide B, amide I, amide II, and amide III. The amide A band of fin, skin, notochord, and cartilage collagen was 3326.36, 3290.14, 3293.34, and 3283.22 cm^{-1}, respectively. The amide A band of porcine skin and bovine cartilage collagen was 3304.35 and 3300.23 cm^{-1}, respectively. Muyonga et al. reported that the absorption band of amide A, associated with N-H stretching vibration [46]. The amide B band of fin, skin, notochord, and cartilage collagen was observed at 2931.10, 2947.55, 2933.68, and 2927.90 cm^{-1}, respectively. The amide B

band of porcine skin and bovine cartilage collagen was observed at 2935.82 and 2933.76 cm^{-1}, respectively. It was associated with the asymmetrical stretching of CH_2. The amide I band frequencies from 1600 to 1700 cm^{-1} were mainly related to carbonyl group stretching vibrations and were characteristic of the secondary coil structure [47]. The amide I bond of fin, skin, notochord, and cartilage collagen was observed at 1658.96, 1661.35, 1631.48, and 1633.41 cm^{-1}, respectively. The amide I bond of porcine skin and bovine cartilage collagen was observed at and 1628.50 and 1630.56 cm^{-1}, respectively. This observation confirmed the formation of hydrogen bonds between N-H stretch, where the C-O residues were responsible for stabilizing the triple helical structure [46]. The amide II and III of fin, skin, notochord, and cartilage collagen were observed at 1453.92, 1452.80, 1547.60, and 1541.81 cm^{-1}; 1239.56, 1239.76, 1238.08, and 1236.15 cm^{-1}, respectively. The amide II and III of porcine skin and bovine cartilage collagen were observed at 1548.20 and 1546.15; 1237.33 and 1237.32 cm^{-1}, respectively. The amide II band corresponded to N-H bending vibration, and the amide III band represented C-H stretching [47]. The FTIR spectra of all collagens were consistent with the structural properties of collagen.

Solubility of collagen

Collagen molecules have the minimum solubility at their isoelectric point and therefore suitable for fibril formation *in vitro* [48]. To discuss the suitable pH condition for fibril-forming, the influence of pH on collagen molecule solubility was investigated as shown in Fig. 3. For fin collagen (Fig. 3-a), the highest solubility appeared at pH 2. The solubility significantly decreased with pH value increasing to 6. The minimum solubility of fin collagen appeared at pH value between 6 and 8. It indicated that the isoelectric point of fin collagen was between pH 6 to 8. A slight increase in solubility was found at pH values of 8 to 12. When the pH value increased to 12, the solubility of fin collagen was dramatically

331 rose to 63.0%. The reason for the high solubility of collagen on the alkaline side might be due to the pH
332 being far from its isoelectric point. For skin collagen (Fig. 3-b), it solubilized to a greater extent in the
333 acidic pH range from 2 to 3. The solubility significantly decreased with pH value increased to 8. The
334 minimum solubility of skin collagen appeared at pH values between 6 to 8. It indicated that the
335 isoelectric point of skin collagen was between pH 6 to 8. When the pH value increased to 10, the
336 solubility of skin collagen rose sharply to 51.1%. It suggested that the solubility of skin collagen was
337 more sensitive to pH change to alkaline side than that of fin collagen.
338 Cartilage collagen (Fig. 3-d) solubilized to a greater extent in the acidic pH range from 2 to 3. The
339 solubility significantly decreased with pH value increasing to 10. The minimum solubility of cartilage
340 collagen appeared at pH values between 8 and 10. It indicated that the isoelectric point of cartilage
341 collagen was between pH 8 and 10. When the pH value increased to 12, the solubility of cartilage
342 collagen was dramatically rose to 78.3%. For notochord collagen (Fig. 3-c), the highest solubility
343 appeared at pH 2. The solubility of notochord collagen was more sensitive to pH change than that of
344 cartilage collagen. As pH value increased to 6, the solubility sharply decreased to 0.57%. A slight
345 increase in solubility was found at alkaline pH values of 8 to 10. It suggested that the isoelectric point
346 of notochord collagen was between pH 6 and 8. Like cartilage collagen, the solubility of notochord
347 collagen increased rapidly with increasing pH value to 12. The solubility results indicated that there
348 were differences in the molecular properties and conformations of the four collagens. Furthermore,
349 amino acid composition is also a non-negligible factor that affects the protein isoelectric point, which
350 in turn affects protein solubility [49].
351 The solubility of collagen with changes in pH may play a crucial role in its extraction method. So
352 far, many studies have discussed the effect of different pH values from 1 to 10 on type I collagen

353 solubility [31]. In this study, we found for the first time that the solubility of sturgeon collagen
354 increased, when the pH was increased to 12. It suggested that part of the collagen molecules could be
355 dissolved in alkaline solution. In our previous study, we reported that sturgeon collagen was lost during
356 the alkaline pretreatment [8]. This result was consistent with the results of collagen solubility,
357 indicating that the alkali-soluble collagen was presented in the sturgeon by-products. Therefore,
358 although alkaline pretreatment can improve collagen extraction efficiency, the conditions of the
359 alkaline pretreatment need to be considered to avoid more collagen loss.

360 **Collagen fibril formation *in vitro***

361 In general, collagen fibril-forming process is divided into three phases: lag phase (no turbidity
362 changes), growth phase (turbidity increasing), and plateau phase (turbidity stabilization) [13]. The
363 progression of fin and skin collagen fibril-forming at different phosphate ion concentrations was shown
364 in Fig. 4 (a and b). When the phosphate ion concentration of solution was 30 mM, the turbidity curves
365 of the two collagens were similar, with no lag phase. At 120 mM phosphate ion concentration, the
366 turbidity of both two collagens did not change. It indicated that collagen fibrils were not formed at 120
367 mM phosphate ion concentration. The effect of phosphate ion concentration on skin collagen fibril-
368 forming were consistent with our previous studies [13]. Significant differences between fin and skin
369 collagen turbidity curves occurred at 60 mM phosphate ion concentration. At this condition, the
370 turbidity curve of fin collagen contained a long lag phase and a smooth growth phase. The plateau
371 phase was not observed after 1 h reaction. For skin collagen, after a short lag phase, a steep growth
372 phase was observed with a rapid increase in turbidity value to near 2. In our previous study, we
373 demonstrated that high phosphate ion concentration inhibited the fibril-forming of sturgeon type I
374 collagen [13]. The inhibitory effect of phosphate ion concentration on fin collagen fibril-forming was

more significant than that of skin collagen. During collagen fibril-forming, linear aggregation of collagen molecules occurred in the lag phase to form subfibrillar units. These subfibrillar units aggregate laterally in the growth phase to form fibrils [50]. The turbidity curve results indicated that, at high phosphate ion concentration, fin collagen needed longer time to form subfibrillar units and was more difficult to self-assemble into thick fibrils than skin collagen. The rate of fibril-forming was mainly controlled by intermolecular interaction between collagen molecules [51]. The progression of porcine skin type I collagen fibril-forming at different phosphate ion concentrations was shown in Fig. 4-c. The turbidity changes of porcine skin type I collagen only appeared at 30 mM phosphate ion concentration. The turbidity increasing of porcine skin type I collagen was much slower than sturgeon type I collagen. It indicated that the fibril-forming ability of sturgeon type I collagen was higher than that of porcine skin type I collagen.

Type II collagen took more time to self-assemble into fibrils than type I collagen. Notochord and cartilage collagens could only form fibril at 30 mM phosphate ion concentration (Fig. 4 c and d). As phosphate ion concentration increased to 60 mM, the turbidity of both two collagens did not change. It indicated that type II collagen could only form fibrils at low phosphate ion concentration compared to type I collagen. No lag phase with no changes in turbidity was observed in the two turbidity curves. It was because the fibril formation speed was too fast that no lag phase was detected in both two type II collagens. The progression of bovine cartilage type II collagen fibril-forming at different phosphate ion concentrations was shown in Fig. 4-f. The turbidity change trends of sturgeon and bovine type II collagens under different phosphate ion concentration conditions were similar. It suggested that sturgeon and bovine type II collagens had similar fibril-forming ability under the same phosphate ion concentration condition. However, the turbidity curves of bovine and rat type II collagens have been

reported to have a longer lag phase during fibril formation [10, 52]. Long lag phase might be due to the different ionic environments in solution. The initial turbidity of cartilage collagen started at 0.53, and then the turbidity curve increased slowly with reaction time. The final turbidity of cartilage collagen ended at 0.70. The initial turbidity of notochord collagen was 0.38, and then the turbidity curve rose rapidly in the first 100 min. After that, the rate of turbidity growth slowed down and the final turbidity ended at 0.78. The turbidity change trend of notochord collagen in this study was consistent with that of Bester sturgeon notochord collagen [8]. The difference in absorbance values came from the amount of collagen added. Comparing to cartilage collagen, the notochord collagen formed fibril with a longer growth phase. It suggested that the fibril formation speed of cartilage collagen was faster than that of notochord collagen. Our previous study reported that collagen fibril lateral aggregation occurred during the growth phase, and the final turbidity value reflected fibril thickness [13]. This result indicated that the fibril diameter of notochord collagen was larger than that of cartilage collagen. Different conformations and molecular structures of collagens might be responsible for their different fibril-forming properties.

Fibril formation degree

The degree of fin and skin collagen fibril formation was assessed after 1 h, and the results were shown in Fig. 5 (a and b). When phosphate ion concentration was 30 mM, the fibril formation degree of fin collagen and skin collagen were 93.34 ± 0.23% and 94.93 ± 0.11%, respectively. When phosphate ion concentration was 60 mM, the fibril formation degree of fin collagen and skin collagen were 90.15 ± 1.07% and 94.05 ± 0.71%, respectively. At the same phosphate ion concentration, the fibril formation degree of skin collagen was slightly higher than that of fin collagen. The fibril formation degree of both two collagens decreased with increasing phosphate ion concentration. This trend was consistent with

Bester sturgeon swim bladder and skin type I collagens [13]. The fibril formation degree of skin collagen at 60 mM phosphate ion in this research was much higher than that of Bester sturgeon skin collagen [13]. Different species of sturgeon were thought to be responsible for different skin collagen fibril formation processes.

The degree of notochord and cartilage collagen fibril formation was assessed by 10 h fibrillogenesis, and the results were shown in Fig. 5 (c). Both notochord and cartilage collagens showed high fibril formation degree with values of 95.13 ± 0.15% and 98.32% ± 0.03%, respectively. It meant that almost all collagen molecules re-assembled into collagen fibrils after 10 h reaction. The degree of fibril formation in notochord collagen was consistent with that of Bester sturgeon notochord collagen [13].

Fibril diameter and morphology

SEM images of fin and skin collagen fibrils formed after incubation for 1 h were shown in Fig. 6, while the diameter distributions of the fibrils were shown in Fig. 8 (a and b). For both collagens, fibril diameter became thicker with increasing phosphate ion concentration in solution. This trend was consistent with the sturgeon swim bladder type I collagen reported in our previous study [13]. Increasing the magnification of the SEM observation in this study showed the fibrillar morphology more clearly than our previous results. At 30 mM phosphate ion concentration, the thick fibrils appeared in both fin and skin collagen fibrils. Many oriented long fibrils were interlaced with thin fibrils. The mean fibril diameter for fin and skin collagen was 58.0 and 60.7 nm, respectively. At a phosphate ion concentration of 60 mM, the mean fibril diameter for fin and skin collagen was 154.9 and 209.0 nm, respectively. The range of the fibril diameter increased significantly comparing with at 30 mM phosphate ion concentrations. There were no fibrils less than 50 nm in diameter throughout the

fibrillar structure, and the maximum diameter of fin and skin collagen fibrils were 334 and 477 nm, respectively. The fibril morphology and diameter results suggested that the phosphate ion concentration had a certain influence on the morphology of sturgeon fin collagen fibrils. However, unlike skin collagen, fin collagen could not be formed thick fibrillar structure even at high phosphate ion concentration. Sturgeon fin collagen could only form fine fibrils *in vitro*. From Fig. 6 (a-1 and a-2 60 mM PB), we found a special dense network structure interlaced with the fibrils and attached to the surface of the fibrils. These special structures formed steric hindrance and inhibited the aggregation of collagen fibrils into thick fibrils. It might be the reason for that fin collagen fibrils were much thinner than skin collagen fibrils. From this study, the exact composition of these dense network structures was not known. Combined with the discussion in the SDS-PAGE section, we speculated that these special structures might be composed of other collagens. Histochemistry method and molecular analyses will be used to demonstrated this hypothesis in our further study. Another characteristic of fibrils under this condition was that a transverse periodic band pattern structure could be observed on fin and skin collagen fibrils. It is well known that the 67 nm D-periodic band pattern is the characteristic of the natural type I collagen fibril *in vivo* [53]. To investigate whether these periodic band patterns resemble the structure of native collagen fibrils *in vivo*, detailed observation of the fibrils using transmission electron microscopy is required in further studies.

In Fig. 6 (b-2 60 mM PB), the ends of the thick fibrillar structure were clearly observed in the skin collagen fibrils (as shown by the white arrow). The tip of the fusiform structure consisted of several skin collagen fibrils. The coarse fibrils were formed by random parallel convergence of several fine fibrils. This process occurred during the growth phase, and many long fibrils accumulated into thick fibrils, resulting in a rapid increase in the turbidity of the solution. Our previous study showed that the

463 thick fusiform structure was found in the swim bladder collagen fibrils at 60 mM phosphate ion
464 concentration, but the structure of the tip of the fusiform was not observed clearly [13]. In this research,
465 we increased observation magnification of SEM and clearly observed the structural properties of the
466 fusiform fibril.

467 SEM images of the notochord and cartilage collagen fibrils after 10 h of incubation were shown in
468 Fig. 7. The diameter distributions of the fibrils were shown in Fig. 8 (c and d). The mean fibril
469 diameters of notochord and cartilage collagens were 52.0 nm and 37.3 nm, respectively. The diameter
470 distribution of notochord collagen fibrils ranged from 11 to 157 nm. The fibrils with diameters less than
471 75 nm accounted for 83.3% of the total fibrils. The diameter distribution of cartilage collagen fibrils
472 ranged from 9 to 127 nm, and the fibrils with diameters less than 50 nm accounted for 77.2% of the
473 total fibrils. Overall, notochord collagen fibrils contained more thick fibrils than cartilage collagen
474 fibrils. Weiss et al. reported that type II collagen fibrils in human articular cartilage have diameters in
475 the range of 40-80 nm [54]. It suggested that the re-assembled fibrils of sturgeon notochord and
476 cartilage type II collagens had a similar thickness degree to native human cartilage fibrils.

477 The unordered, net-like appearance of fine fibrils exhibited in both notochord and cartilage
478 collagen fibrils (Fig 8 a-1 and b-1). Comparing to cartilage collagen fibrils, notochord collagen fibrils
479 contained more thick fusiform structure interwoven with fine fibrils (white arrows in Fig 8 b-2 and b-
480 3). These special fusiform structures enable notochord collagen fibrils had a higher fibril diameter
481 distribution than cartilage collagen fibrils. As shown by white arrows in Fig. 7 b-3, the thick fusiform
482 structure was formed by the accumulation of many fine fibrils. This result was consistent with the
483 result of turbidity curve. During the long growth phase of notochord collagen, more fine fibrils
484 accumulated into thick fibrils. The formation of fibrils with different morphology might be due to the

485 presence of a small amount of type I collagen in cartilage collagen. In our previous study, we
486 demonstrated that the amino acid compositions were different between type I and type II collagens [8].
487 Therefore, the molecular conformations of two types collagens were also different. The formation of
488 collagen fibrils *in vitro* was a highly regular self-assembly process. The presence of type I collagen
489 might cause steric hindrance to the regular self-assembly process of type II collagen molecules. Lapiere
490 et al. reported that the addition of other collagens reduced the lateral aggregation of type I collagen
491 fibrils, resulting in the formation of fine fibril networks [55]. Adachi & Hayashi also reported that type
492 V collagen restricted the growth of type I collagen fibrils to thick fibrils *in vitro* [56]. To our best
493 knowledge, till now there was no similar studies on type II collagen fibril formation. Here we
494 hypothesis that the presence of type I collagen will affect the fibril-forming process and fibril
495 morphology of cartilage type II collagen. In our further study, pure type I and type II collagens will be
496 used to demonstrate this hypothesis.

497 **Yields and molecular distribution of collagen peptides**

498 Papain was a plant-derived protease for food processing. In our recent study, Li et al demonstrated that
499 papain hydrolysates of skate cartilage had higher antioxidant activity and lower molecular weight than
500 other protease hydrolysates (such as trypsin, chymotrypsin, and pepsin) [57]. In addition, papain is
501 comparatively less expensive than the other proteolytic enzymes [57]. Considering the production
502 efficiency and the cost for large-scale production, we used papain to treat four sturgeon collagens in
503 this study. The yields of collagen peptides for fin, skin, notochord, and cartilage were 78.8%, 99.1%,
504 74.2%, and 89.2%, respectively. The SDS-PAGE of collagen peptides was shown in Fig. 9. Notochord
505 collagen peptide was smeared after CBB staining with no clear bands, whereas other collagen peptides
506 showed several bands at molecular weight above 17 kDa. Cartilage collagen peptide showed two bands

at molecular weight above 24 kDa. It suggested that notochord collagen peptide had more low molecular peptides compared to the other three collagen peptides, while cartilage collagen peptide had more high molecular weight peptides. Except for notochord collagen peptide, the other three collagen peptides had a smearing area on the SDS-PAGE. The smearing area was an aggregate of collagen peptides with similar molecular weight. It also indicated that the molecular weight of notochord collagen peptide was lower than that of the other three collagen peptides.

Antioxidant activity of collagen peptides

Among the ROS generated in an animal body, the hydroxyl radical is the primary active oxygen species with the strongest reactivity. Therefore, the scavenging of hydroxyl radicals is one of the most effective defense mechanisms of a living body against various diseases. Hydroxyl radical scavenging activity of the collagen peptides was summarized in Fig. 10-a. The activities of all collagen peptides increased in concentration-dependent manners. At the same concentration, the Hydroxyl radical scavenging activity of the four collagen peptides was notochord > skin > fin > bovine cartilage > porcine skin > cartilage. The antioxidant activity of notochord collagen peptide was higher than that of Vc, when the sample concentration was 5 mg/mL.

ABTS radical scavenging activity of collagen peptides was shown in Fig. 10-b. All collagen peptides showed ABTS radical scavenging activity in a dose-dependent manner. At the same concentration, the ABTS radical scavenging activity order of the four collagen peptides was skin > notochord > fin > bovine cartilage > cartilage > porcine skin. Although the molecular weight of notochord collagen peptide was lower than that of skin collage peptides, the antioxidant activity of skin collagen peptide was higher than that of notochord collagen peptides. It suggested that the antioxidant activity of collagen peptides was not only related to the molecular weight of peptides. The results of

two free radical scavenging activities also showed that the antioxidant activity of collagen peptides was directly related to collagen type. Comparing with the other two sturgeon by-products, the skin and notochord was more suitable for producing antioxidant collagen peptide.

Conclusions

The present study was the first to clarify the collagen structural characteristics of collagens, which extracted from four Russian sturgeon by-products. Meanwhile, the biological properties of the four collagens were compared through the fibril formation ability of the collagen molecule and the antioxidant activity of the collagen peptide. The α-chain pattern results indicated that the main collagen of fin and skin was type I collagen, and the main collagen of notochord and cartilage was type II collagen. The solubility results of collagen at different pH suggested that the isoelectric points of the skin, fin, and notochord collagens were approx. in the pH range of 6 to 8. Notochord and cartilage type II collagen could only self-assemble into fibril at low phosphate ion concentration condition, while skin and fin type I collagen could self-assemble into fibril at a wide range of phosphate ion concentration. The fibrillar morphology of type I collagen was more diversified than that of type II collagen. Under the same hydrolysis of papain, the molecular weight of notochord collagen peptide was lower than that of the other three collagen peptides. The antioxidant activity of notochord and skin collagen peptide was better than that of the other collagen peptides. Since there is no previous study on the utilization of Russian sturgeon collagen, this study will provide basic data for the application of Russian sturgeon collagen in the food and biomedical material industries. Meanwhile, the effective utilization of collagen will be a feasible way to increase the value of Russian sturgeon by-products.

Acknowledgements

The authors would like to thank Key Lab of Freshwater Biodiversity Conservation, Yangtze River

Fisheries Research Institute; Zhejiang Province Joint Key Laboratory of Aquatic Products Processing, Zhejiang Gongshang University, for their financial and instrumentation support in the development of this study. Thanks for Prof. Yasuaki Takagi of Faculty of Fisheries Sciences, Hokkaido University supply to technical support and article modification.

References

1. Birstein, V. J., Bemis, W. E., Waldman, J. R.: The threatened status of acipenseriform species: A summary. Environ. Biol. Fish. **48**, 427-435 (1997).

2. Tavakoli, S., Luo, Y. K., Regenstein, J. M., Daneshvar, E., Bhatnagar, A., Tan, Y. Q., Hong, H.: Sturgeon, Caviar, and Caviar Substitutes: From Production, Gastronomy, Nutrition, and Quality Change to Trade and Commercial Mimicry. Rev. fish. Sci. Aquac. **29**, 753-768 (2021).

3. Bronzi, P., Chebanov, M., Michaels, J. T., Wei, Q. W., Rosenthal, H., Gessner, J.: Sturgeon meat and caviar production: Global update 2017. J. Appl. Ichthyol. **35**, 257-266 (2019).

4. Hurvitz, A., Jackson, K., Degani, G., Levavi-Sivan, B.: Use of endoscopy for gender and ovarian stage determinations in Russian sturgeon *(Acipenser gueldenstaedtii)* grown in aquaculture. Aquaculture. **270**, 158-166 (2007).

5. Chen, Y. W., Cai, W. Q., Shi, Y. G., Dong, X. P., Bai, F., Shen, S. K., Jiao, R., Zhang, X. Y., Zhu, X.: Effects of different salt concentrations and vacuum packaging on the shelf stability of Russian sturgeon *(Acipenser gueldenstaedti)* stored at 4 °C. Food. Control. **109**, 106865 (2020).

6. Meng, D. W., Leng, X. Q., Zhang, Y., Luo, J., Du, H., Takagi, Y., Dai, Z. Y., Wei, Q. W.: Comparation of the structural characteristics and biological activities of chondroitin sulfates extracted from notochord and backbone of Chinese sturgeon *(Acipenser sinensis)*. Carbohydr. Res. **522**, 108685 (2022).

573 7. Zhang, X., Ookawa, M., Tan, Y. K., Ura, K., Adachi, S., Takagi, Y.: Biochemical characterisation and
574 assessment of fibril-forming ability of collagens extracted from Bester sturgeon *Huso huso* ×
575 *Acipenser ruthenus*. Food. Chem. **160**, 305-312 (2014).
576 8. Meng, D. W., Tanaka, H., Kobayashi, T., Hatayama, H., Zhang, X., Ura, K., Yunoki, S., Takagi, Y.:
577 The effect of alkaline pretreatment on the biochemical characteristics and fibril-forming abilities of
578 types I and II collagen extracted from bester sturgeon by-products. Int. J. Biol. Macromol. **131**, 572-
579 580 (2019).
580 9. Strueuli, C.: Extracellular matrix remodelling and cellular differentiation. Curr. Opin. Cell. Biol. **11**,
581 634-640 (1999).
582 10. Silver, F. H., Freeman, J. W., Seehra, G. P.: Collagen self-assembly and the development of tendon
583 mechanical properties. J. Biomech. **36**, 1529-1553 (2003).
584 11. Kim, S. K., Mendis, E.: Bioactive compounds from marine processing byproducts – A review. Food.
585 Res. Int. **39**, 383-393 (2006).
586 12. Alves, A. L., Marques, A. L. P., Martins, E., Silva, T. H., Reis, R. L.: Cosmetic potential of marine
587 fish skin collagen. Cosmetics. **4**, 4040039 (2017).
588 13. Meng, D. W., Li, W., Ura, K., Takagi, Y.: Effects of phosphate ion concentration on in-vitro
589 fibrillogenesis of sturgeon type I collagen. Int. J. Biol. Macromol. **148**, 182-191 (2020).
590 14. Curtis, A. S. G., Clark, P.: The effects of topographic and mechanical properties of materials on cell
591 behavior. Crit. Rev. Biocompat. **5**, 343-362 (1990).
592 15. Ahmed, M., Verma, A. K., Patel, R.: Collagen extraction and recent biological activities of collagen
593 peptides derived from sea-food waste: A review. Sustain. Chem. Pharm. **18**, 100315 (2020).
594 16. Taghvaei, M., Jafari, S.M., Mahoonak, A. S., Nikoo, A.M., Rahmanian, N., Hajitabar, J., Meshginfar,

595 N.: The effect of natural antioxidants extracted from plant and animal resources on the oxidative
596 stability of soybean oil. LWT-Food. Sci. Technol. **56**, 124-130 (2014).
597 17. Mahapatra, S., Chakraborty, S., Majumdar, S., Bag, B., Roy, S.: Eugenol protects nicotine-induced
598 superoxide mediated oxidative damage in murine peritoneal macrophages *in vitro*. Eur. J. Pharmacol.
599 **623**, 132-140 (2009).
600 18. Zhao, X. C., Zhang, X. J., Liu, D. Y.: Collagen peptides and the related synthetic peptides: A review
601 on improving skin health. J. Funct. Foods. **86**, 104680 (2021).
602 19. Sheng, Y., Qiu, Y. T., Wang, Y. M., Chi, C. F., Wang, B.: Novel antioxidant collagen peptides of
603 Siberian Sturgeon *(Acipenser baerii)* cartilages: the preparation, characterization, and
604 cytoprotection of H_2O_2-damaged human umbilical vein endothelial cells (HUVECs). Mar. Drugs.
605 **20**, 325 (2022).
606 20. Nikoo, M., Benjakul, S., Xu, X. M.: Antioxidant and cryoprotective effects of Amur sturgeon skin
607 gelatin hydrolysate in unwashed fish mince. Food. Chem. **181**, 295-303 (2015).
608 21. Clowacki, J., Mizuno, S.: Collagen scaffolds for tissue engineering. Biopolymers. **89**, 338-344 (2007).
609 22. Nalinanon, S., Benjakul, S., Visessanguan, W., Kishimura, H.: Use of pepsin for collagen extraction
610 from the skin of bigeye snapper *(Priacanthus tayenus)*. Food. Chem. **104**, 593-601 (2007).
611 23. Meng, D. W., Li, W., Leng, X. Q., Takagi, Y., Dai, Z. Y., Du, H., Wei, Q. W.: Extraction of chondroitin
612 sulfate and type II collagen from sturgeon *(Acipenser gueldenstaedti)* notochord and
613 characterization of their hybrid fibrils. Process. Biochem. **124**, 180-188 (2023).
614 24. Laemmli, U. K.: Cleavage of structural proteins during the assembly of the head of bacteriophage T4.
615 Nature. **277**, 680–685 (1970).
616 25. Atef, M., Ojagh, S. M., Latifi, A. M., Esmaeili, M., Udenigwe, C. C.: Biochemical and structural

617 characterization of sturgeon fish skin collagen (Huso huso). J. Food. Biochem. **44**, e13256 (2020).
618 26. Lowry, O. H., Rosebrough, N. J., Farr, A. L., R. Randall, J.: Protein measurement with the folin
619 phenol reagent. J. Biol. Chem. **193**, 265–275 (1951).
620 27. Pan, X., Zhao, Y., Hu, F., Wang, B.: Preparation and identification of antioxidant peptides from
621 protein hydrolysate of skate *(Raja porosa)* cartilage. J. Funct. Foods. **25**, 220-230 (2016).
622 28. Re, R., Pellegrini, N., Proteggente, A., Pannala, A., Yang, M., Rice-Evans, C.: Antioxidant activity
623 applying an improved ABTS radical cation decolorization assay, Free Radic. Biol. Med. **26**, 1231-
624 1237 (1999).
625 29. Nagai, T.: Characterization of collagen from Japanese sea bass caudal fin as waste material. Eur.
626 Food. Res. Technol. **218**, 424-427 (2004).
627 30. Liu, D. S., Liang, L., Regenstein, J. M., Zhou, P.: Extraction and characterisation of pepsin-solubilised
628 collagen from fins, scales, skins, bones and swim bladders of bighead carp *(Hypophthalmichthys*
629 *nobilis)*. Food. Chem. **133**, 1441-1448 (2012).
630 31. Foegeding, E. A., Lanier, T. C., Hultin, H. O.: Food. Chem, ed. by Fennema OR. New York, Marcel
631 Dekker Inc, pp. 902-906 (1996).
632 32. Saito, M., Takenouchi, Y., Kunisaki, N., Kimura, S.: Complete primary structure of rainbow trout
633 type I collagen consisting of α1 (I) α2 (I) α3 (I) heterotrimers. Eur. J. Med. Chem. **268**, 2817-2827
634 (2001).
635 33. Zhang, X., Adachi, S., Ura, K., Takagi, Y.: Properties of collagen extracted from Amur sturgeon
636 *Acipenser schrenckii* and assessment of collagen fibrils in vitro. Int. J. Biol. Macromol. **137**, 809-
637 820 (2019).
638 34. Liang, Q. F., Wang, L., Sun, W. H., Z. Wang, B., Xu, J. M., Ma, H. L.: Isolation and characterization

639 of collagen from the cartilage of Amur sturgeon *(Acipenser schrenckii)*. Process. Biochem. **49**, 318-
640 323 (2014).
641 35. Li, S. W., Prockop, D. J., Helminen, H., Fassler, R., Lapvetelainen, T., Kiraly, K., Peltarri, A.,
642 Arokoski, J., Lui, H., Arita, M.: Transgenic mice with targeted inactivation of the Col2 alpha 1 gene
643 for collagen II develop a skeleton with membranous and periosteal bone but no endochondral bone.
644 Gene. Dev. **9**, 2821-2830 (1995).
645 36. Medici, D., Olsen, B. R.: The role of endothelial- mesenchymal transition in heterotopic ossification.
646 J. Bone. Miner. **27**, 1619-1622 (2012).
647 37. Zhang, X., Shimoda, K., Ura, K., Adachi, S., Takagi, Y.: Developmental structure of the vertebral
648 column, fins, scutes and scales in bester sturgeon, a hybrid of beluga *Huso huso* and sterlet
649 *Acipenser ruthenus*. J. Fish. Bio. **81**, 1985-2004 (2012).
650 38. Leprévost, A., Azaïs, T., Trichet, A., Sire, J. Y.: Vertebral development and ossification in the siberian
651 sturgeon *(Acipenser Baerii)*, with new insights on bone histology and ultrastructure of vertebral
652 elements and scutes. The. Anatomical. Record. **300**, 437-449 (2017).
653 39. Viguet-Carrin, S., Garnero, P., Delmas, P. D.: The role of collagen in bone strength. Osteoporosis. Int.
654 **17**, 319-336 (2006).
655 40. Zhang, X., Azuma, N., Hagihara, S., Adachi, S., Ura, K., Takagi, Y.: Characterization of type I and II
656 procollagen α1chain in Amur sturgeon *(Acipenser schrenckii)* and comparison of their gene
657 expression. Gene. **579**, 8-16 (2016).
658 41. Mizuta, S., Asano, C., Yokoyama, Y., Taniguchi, M.: Molecular species of collagen in muscular and
659 vertebral parts of white sturgeon Acipenser transmontanus. Fisheries. Sci. **78**, 399-406 (2012).
660 42. Luo, Q. B., Chi, C. F., Yang, F., Zhao, Y. Q., Wang, B.: Physicochemical properties of acid-and

661 pepsin-soluble collagens from the cartilage of Siberian sturgeon. Environ. Sci. Pollut. R. **25**, 31427-
662 31438 (2018).
663 43. Zhu, L. L., Li, J. W., Wang, Y. C., Sun, X., Li, B. F., Poungchawanwong, S., Hou, H.: Structural
664 feature and self-assembly properties of type II collagens from the cartilages of skate and sturgeon.
665 Food. Chem. **331**, 127340 (2020).
666 44. Sato, K., Ohashi, C., Ohtsuki, K., Kawabata, M.: Type V collagen in trout *(Salmo gairdneri)* muscle
667 and its solubility change during chilled storage of muscle. J. Agri. Food. Chem. **39**, 1222-1225
668 (1991).
669 45. Plepis, A. M. D. G., Goissis, G., Gupta, D. D.: Dielectric and pyroelectric characterization of anionic
670 and native collagen. Polym. Eng. Sci. **36**, 2932-2938 (1996).
671 46. Muyonga, J. H., Cole, C. G. B., Duodu, K. G.: Characterisation of acid soluble collagen from skins
672 of young and adult Nile perch *(Lates niloticus)*. Food. Chem. **85**, 81-89 (2004).
673 47. Veeruraj, A., Arumugam, M., Balasubramanian, T.: Isolation and characterization of thermostable
674 collagen from the marine eel-fish *(Evenchelys macrura)*. Process. Biochem. **48**, 1592-1602 (2013).
675 48. Li, Y. P., Douglas, E. P.: Effects of various salts on structural polymorphism of reconstituted type I
676 collagen fibrils. Colloids. Surf. B. **112**, 42-50 (2013).
677 49. Patrickios, C. S.: Polypeptide amino acid composition and isoelectric point: 1. A closed-form
678 approximation. J. Colloid. Interf. Sci. **175**, 256-260 (1995).
679 50. Kalbitzer, L., Pompe, T.: Fibril growth kinetics link buffer conditions and topology of 3D collagen I
680 networks. Acta. Biomater. **67**, 206-214 (2018).
681 51. Shi, L. F., Tian, H. H., Wang, Y. X., Hao, G. X., Chen, J., Weng, W. Y.: Effect of pH on properties of
682 golden pompano skin collagen-based fibril gels by self-assembly *in vitro*. J. Sci. Food. Agr. **100**,

4801-4807 (2020).

52. Birk, D. E., Silver, F. H.: Collagen fibrillogenesis in vitro: comparison of types I, II, and III. Arch. Biochem. Biophys. **235**, 178-185 (1984).

53. Kemp, N. E.: Banding pattern and fibrillogenesis of ceratotrichia in shark fins. J. Morph. **154**, 187-204 (1977).

54. Weiss, C., Rosenberg, L., Helfet, A. J.: An ultrastructural study of normal young adult human articular cartilage. J. Bone. Joint. Surg. Am. **50**, 663-674 (1968).

55. Lapiere, C. M., Nusgens, B., Pierard, G. E.: Interaction between collagen type I and type III in conditioning bundles organization. Connect. Tissue. Res. **5**, 21-29 (1977).

56. Adachi, E., Hayashi, T.: In vitro formation of hybrid fibrils of type V collagen and type I collagen limited growth of type I collagen into thick fibrils by type V collagen. Connect. Tissue. Res. **14**, 257-266 (1986).

57. Li, W., Kobayashi, T., Meng, D. W., Miyamoto, N., Tsutsumi, N., Ura, K., Takagi, Y.: Free radical scavenging activity of type II collagen peptides and chondroitin sulfate oligosaccharides from by-products of mottled skate processing. Food. Biosci. **41**, 100991 (2021).

Statements and Declarations

Funding

This work was partially supported by key laboratory research fund open topics (LFBC1002) from Key Lab of Freshwater Biodiversity Conservation, Ministry of Agriculture and Rural Affairs of China; Fundamental Research Funds for the Provincial Universities of Zhejiang (3090JYN9920001G-307).

Competing Interests

The author declares that he has no conflict of interest.

Author Contribution

All authors had read and agreed with the published version of the manuscript. Dawei Meng: Conceptualization, Methodology, Data curation, Investigation, Writing-original draft. Qiwei Wei: Supervision. Prof. Yasuaki Takagi: Methodology, Writing-review & Editing. Prof. Zhiyuan Dai: Resources. Yan Zhang: Methodology. All authors read and approved the final manuscript.

Data availability

Not applicable.

Fig. 1 SDS-PAGE of collagen. M: Molecular weight marker; Lane 1: fin collagen; Lane 2: skin collagen; Lane 3: notochord collagen; Lane 4: backbone cartilage collagen; Lane 5: porcine skin collagen; Lane 6: bovine cartilage collagen

Fig. 2 Infra-red spectra of the sturgeon (a) fin collagen; (b) skin collagen; (c) notochord collagen; (d) backbone cartilage collagen: (e) porcine skin collagen; (f) bovine cartilage collagen

Fig. 3 Solubility of the sturgeon (a) fin collagen; (b) skin collagen; (c) notochord collagen; (d) backbone cartilage collagen at different pH

Fig. 4 Fibril formation in vitro by (a) fin collagen; (b) skin collagen; (c) porcine skin collagen; (d) notochord collagen; (e) backbone cartilage collagen; (f) bovine cartilage collagen measured by optical absorbance at 320 nm with different PB buffer concentration (30, 60, 120 mM)

Fig. 5 The degree of fibril formation of collagen. (a) fin collagen in 30 mM and 60 mM PB buffer; (b) skin collagen in 30 mM and 60 mM PB buffer; (c) notochord and backbone cartilage collagen in 30 mM PB buffer

727 **Fig. 6** Scanning electron micrographs of sturgeon fin and skin collagen fibrils in 30 mM and 60 mM PB
728 buffer. (a) fin collagen; (b) skin collagen. Scale bars: (1) 10 μm; (2) 1 μm. White arrow in b-2 60
729 mM PB: The fusiform structure at the tip of skin collagen fibril
730 **Fig. 7** Scanning electron micrographs of sturgeon notochord and backbone cartilage collagen fibrils in
731 30 mM PB buffer. (a) notochord collagen; (b) backbone cartilage collagen. Scale bars: (1) 2 μm; (2)
732 2 μm; (3) 0.2 μm. White arrow: Thick fusiform structure of notochord collagen fibril
733 **Fig. 8** Diameter distribution of sturgeon collagen fibril (a) fin collagen fibril in 30 mM and 60 mM PB
734 buffer; (b) skin collagen fibril in 30 mM and 60 mM PB buffer; (c): notochord collagen fibril in 30
735 mM PB buffer; (d) backbone cartilage collagen fibril in 30 mM PB buffer
736 **Fig. 9** SDS-PAGE of sturgeon collagen peptides. M: molecular maker; Lane 1: fin collagen peptide; Lane
737 2: skin collagen peptide; Lane 3: notochord peptide; Lane 4: backbone cartilage peptide.
738 **Fig. 10** Hydroxyl (a) and ABTS (b) radical scavenging activities of collagen peptides.

Four main sturgeon by-products

Structural characteristics

Biological properties

Cartilage

Notochord

Acipenser gueldenstaedti

Collagen extraction

Skin

Fin

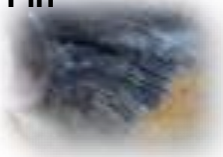

Undenatured collagen (Lyophilized sample)

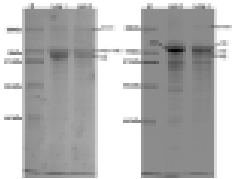

α-chain pattern

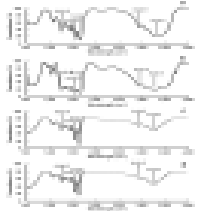

Triple helical structure

High molecular collagen fibril

Fibril forming ability

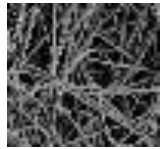

Fibrillar morphology

Low molecular collagen peptides

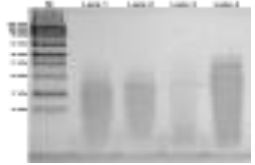

MW distribution

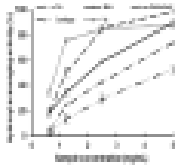

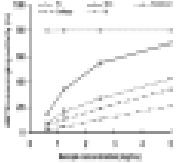

Antioxidant activity

Fig.1

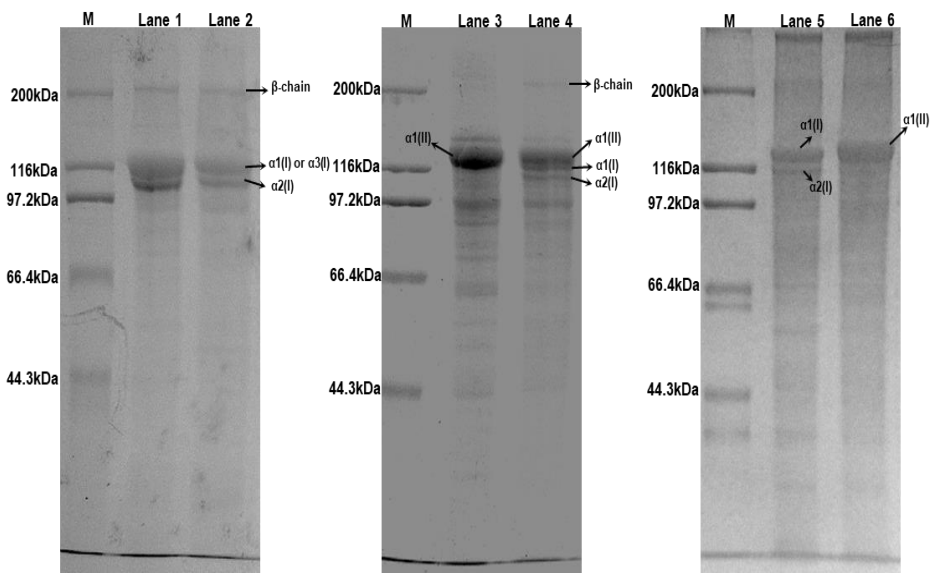
M
Lane 1
Lane 2
200kDa
116kDa
97.2kDa
66.4kDa
44.3kDa
β-chain
α1(I) or α3(I)
α2(I)
M
Lane 3
Lane 4
200kDa
116kDa
97.2kDa
66.4kDa
44.3kDa
α1(II)
β-chain
α1(II)
α1(I)
α2(I)
M
Lane 5
Lane 6
200kDa
116kDa
97.2kDa
66.4kDa
44.3kDa
α1(I)
α2(I)
α1(II)

Fig.2

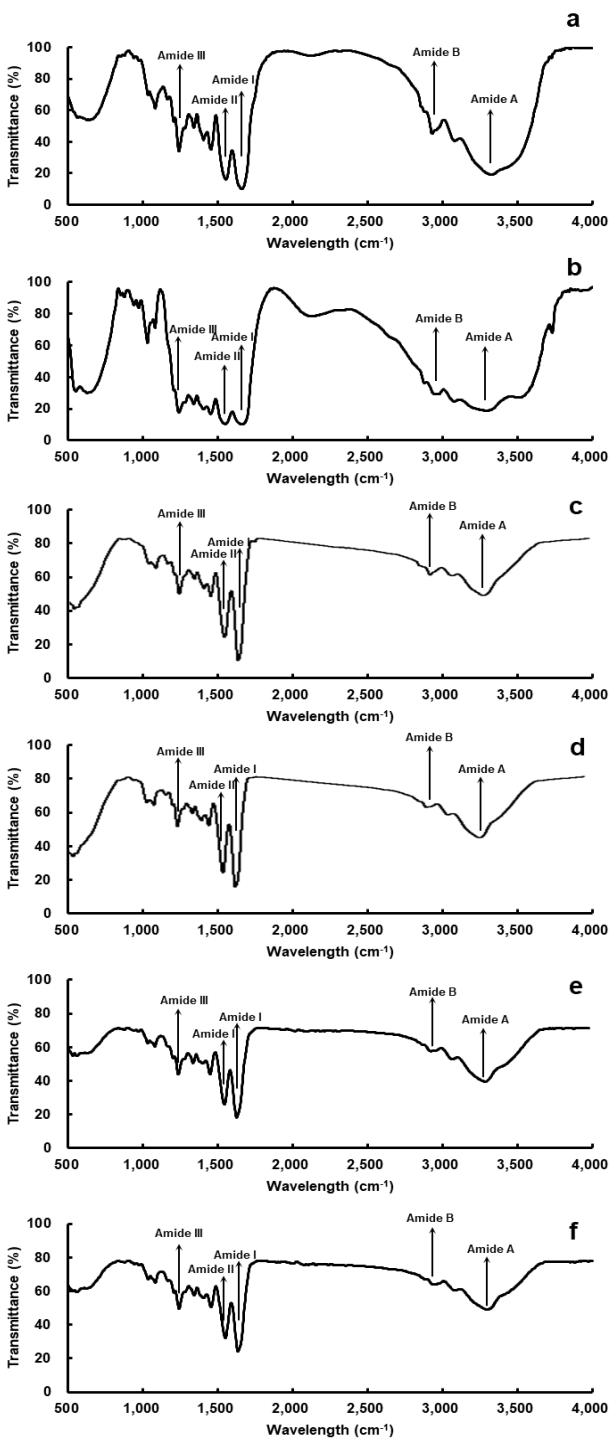
a
b
c
d
e
f
Amide III
Amide I
Amide II
Amide B
Amide A
Transmittance (%)
Wavelength (cm-1)
100
80
60
40
20
0
500
1,000
1,500
2,000
2,500
3,000
3,500
4,000

Fig.3

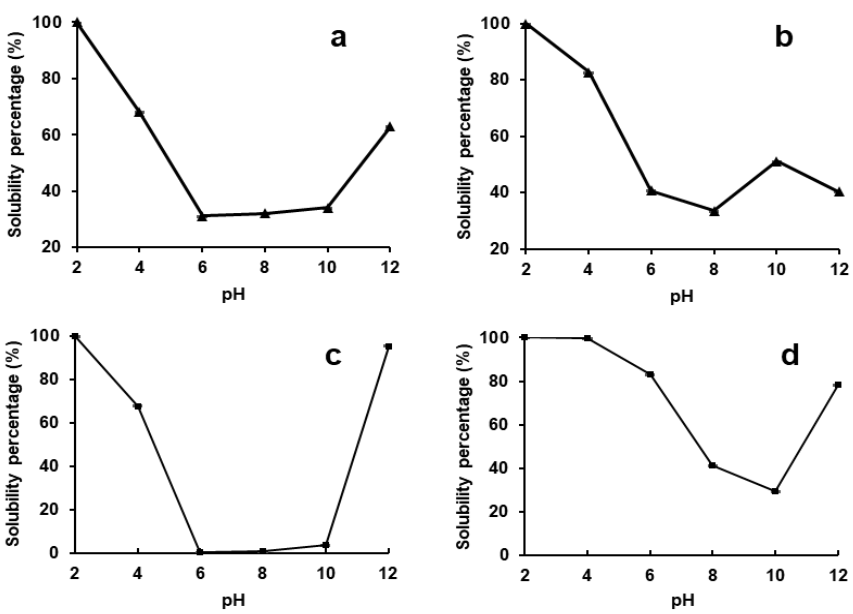

Fig.4

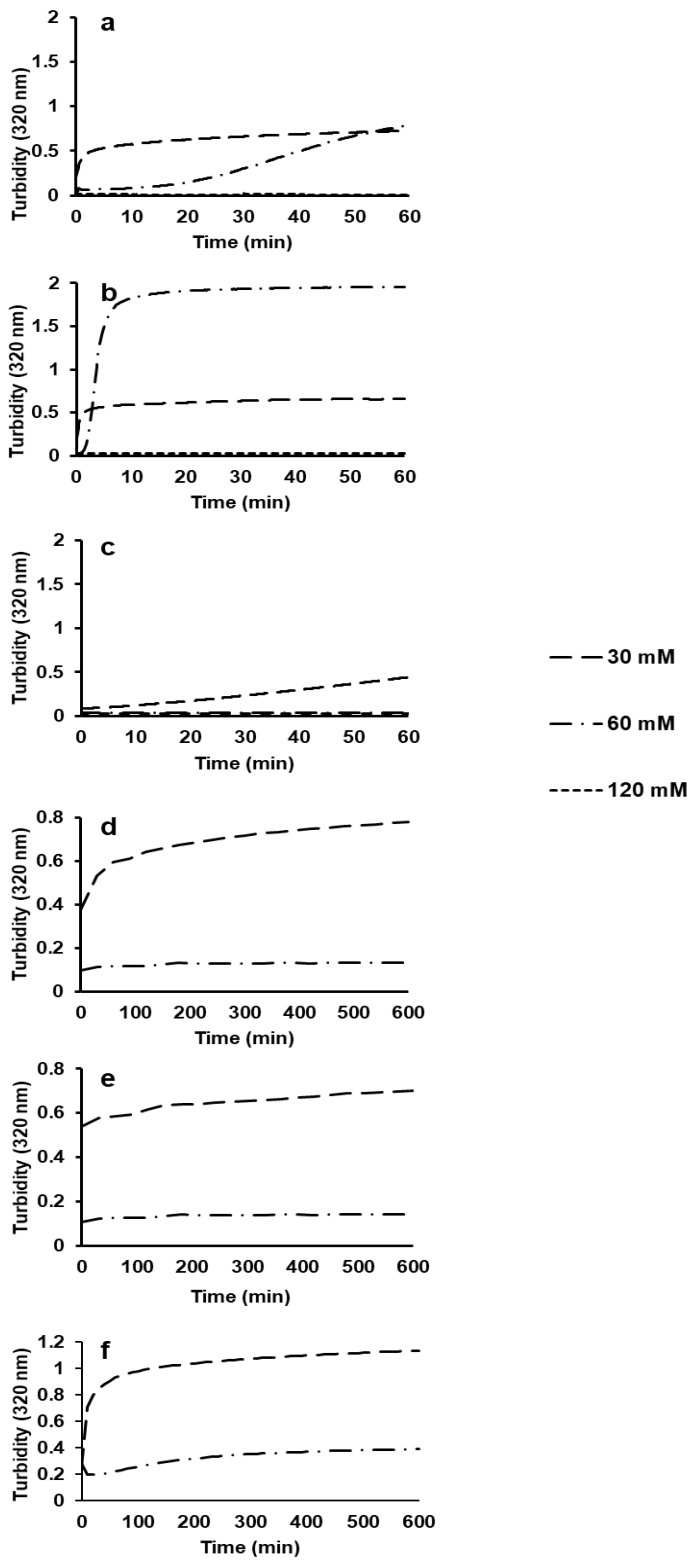

Fig.5

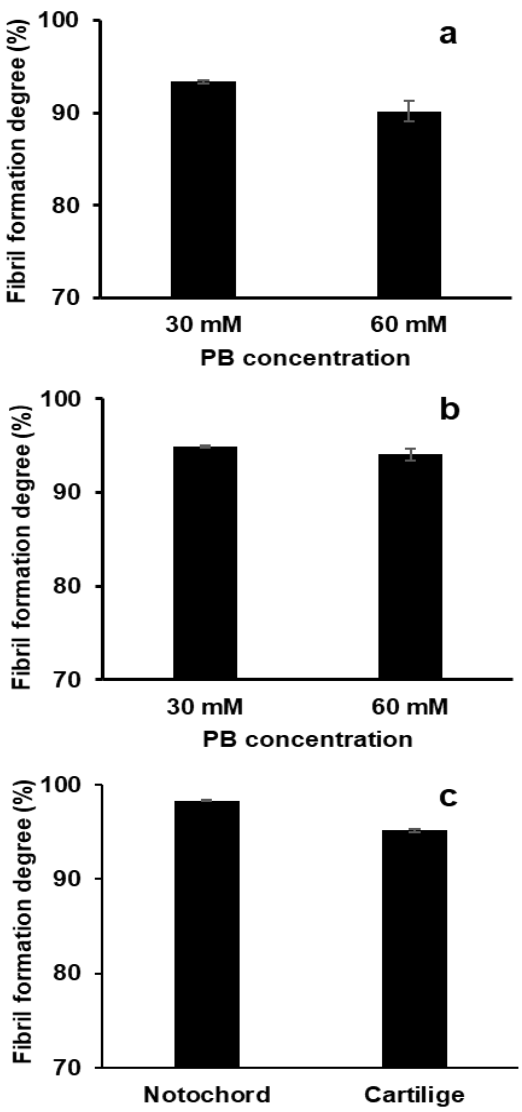
a
Fibril formation degree (%)
100
90
80
70
30 mM
60 mM
PB concentration
b
Fibril formation degree (%)
100
90
80
70
30 mM
60 mM
PB concentration
c
Fibril formation degree (%)
100
90
80
70
Notochord
Cartilige

Fig.6

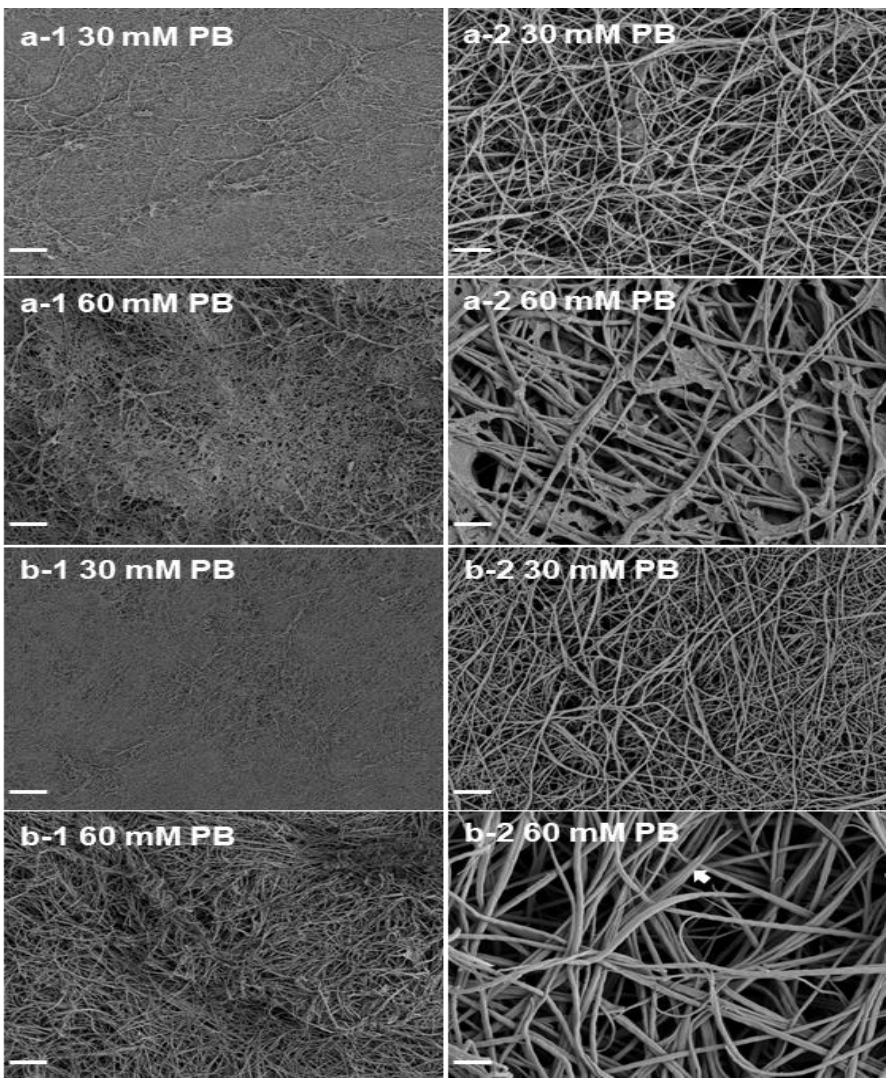
a-1 30 mM PB
a-2 30 mM PB
a-1 60 mM PB
a-2 60 mM PB
b-1 30 mM PB
b-2 30 mM PB
b-1 60 mM PB
b-2 60 mM PB

Fig.7

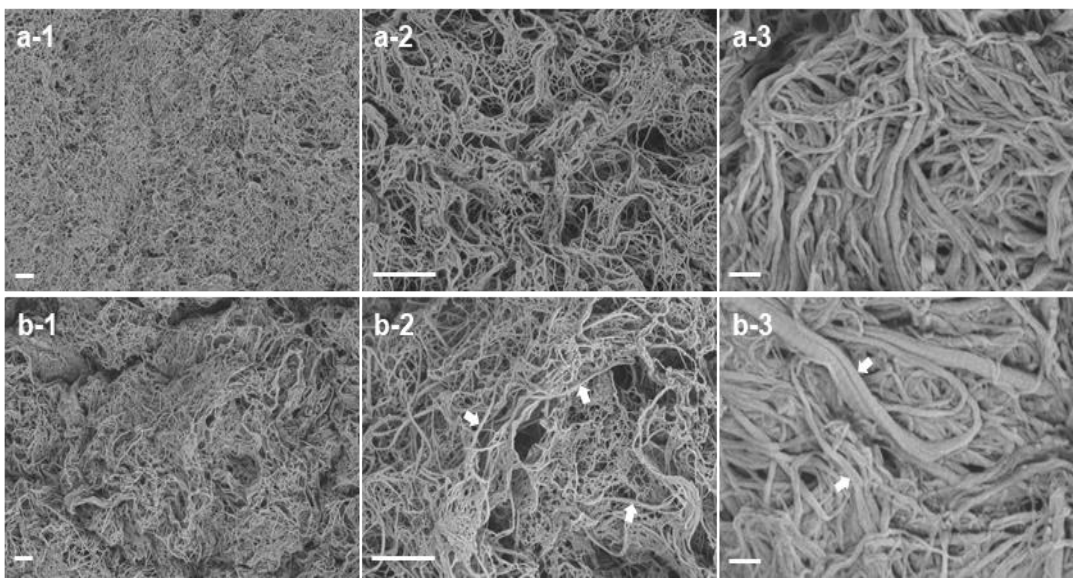

Fig.8

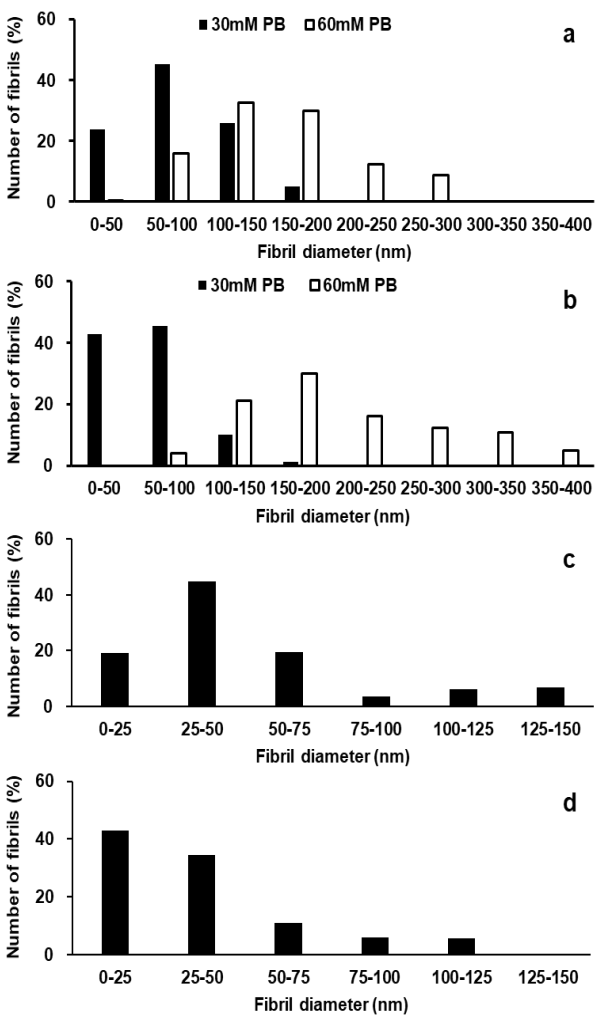
30mM PB
60mM PB
a
Number of fibrils (%)
60
40
20
0
0-50
50-100
100-150
150-200
200-250
250-300
300-350
350-400
Fibril diameter (nm)
30mM PB
60mM PB
b
Number of fibrils (%)
60
40
20
0
0-50
50-100
100-150
150-200
200-250
250-300
300-350
350-400
Fibril diameter (nm)
c
Number of fibrils (%)
60
40
20
0
0-25
25-50
50-75
75-100
100-125
125-150
Fibril diameter (nm)
d
Number of fibrils (%)
60
40
20
0
0-25
25-50
50-75
75-100
100-125
125-150
Fibril diameter (nm)

Fig.9

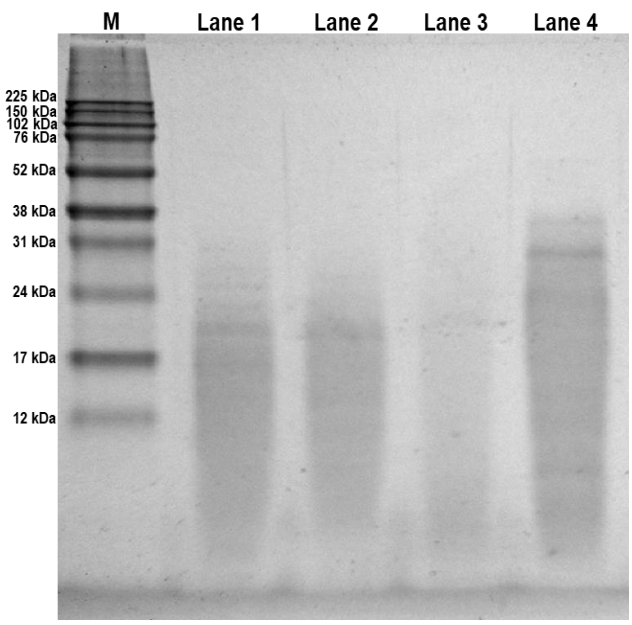
M
Lane 1
Lane 2
Lane 3
Lane 4
225 kDa
150 kDa
102 kDa
76 kDa
52 kDa
38 kDa
31 kDa
24 kDa
17 kDa
12 kDa

Fig.10

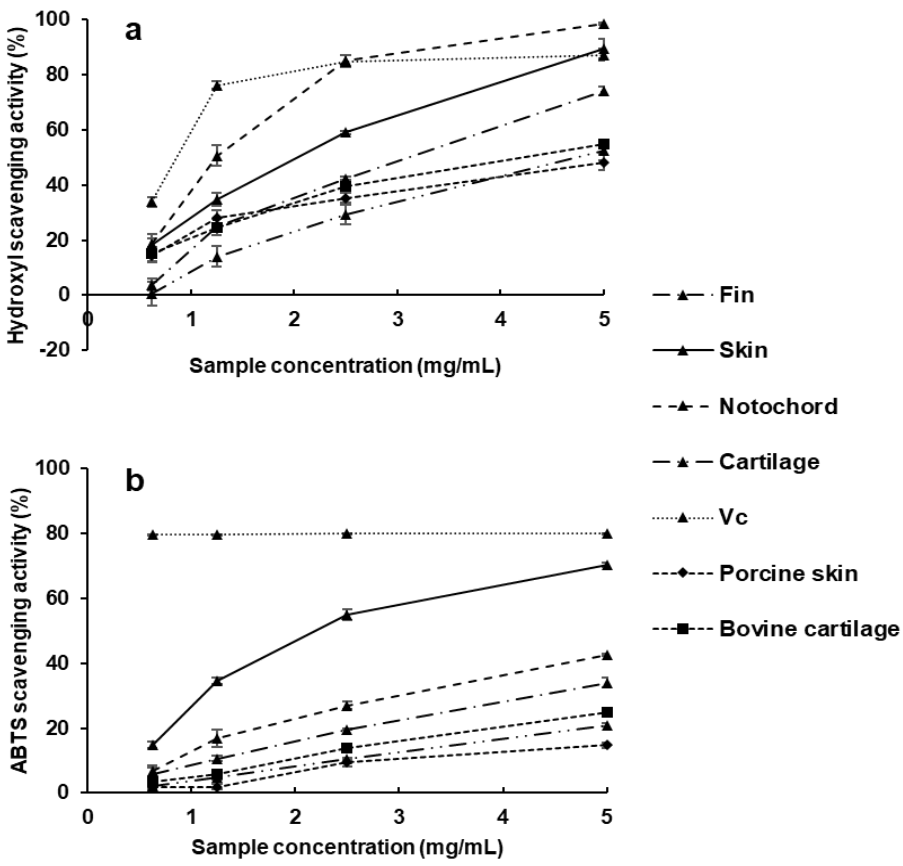
a
Hydroxyl scavenging activity (%)
100
80
60
40
20
0
-20
0
1
2
3
4
5
Sample concentration (mg/mL)
b
ABTS scavenging activity (%)
100
80
60
40
20
0
0
1
2
3
4
5
Sample concentration (mg/mL)
Fin
Skin
Notochord
Cartilage
Vc
Porcine skin
Bovine cartilage